

Figure S1. MS spectrum of C3-3 (A) and MS/MS identification of a peak of m/z 1021.522 (B).

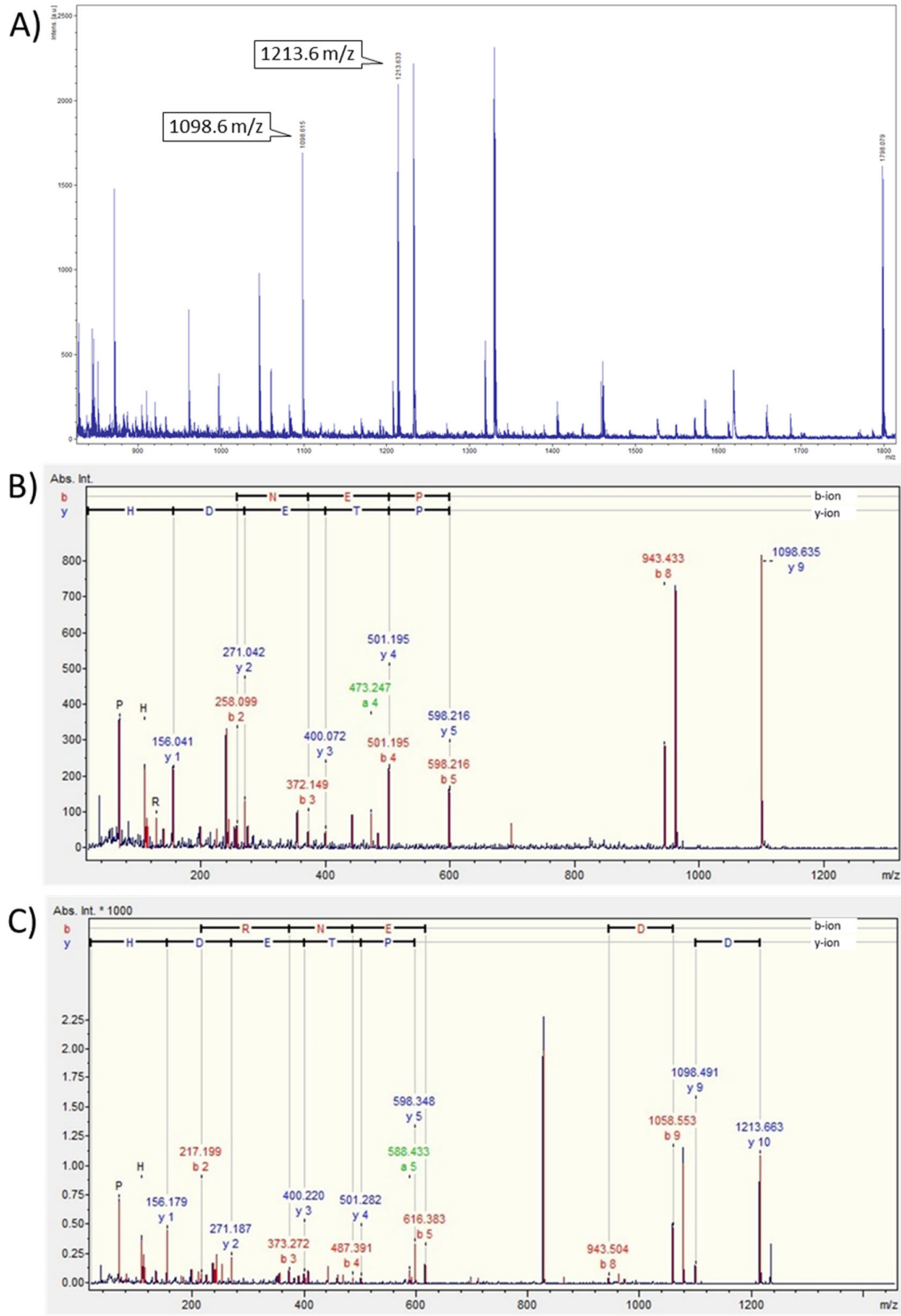


Figure S3. MS spectrum of C3-5 (A) and MS/MS identification of two peaks of *m/z* 1098.615 (B) and 1213.633 (C).

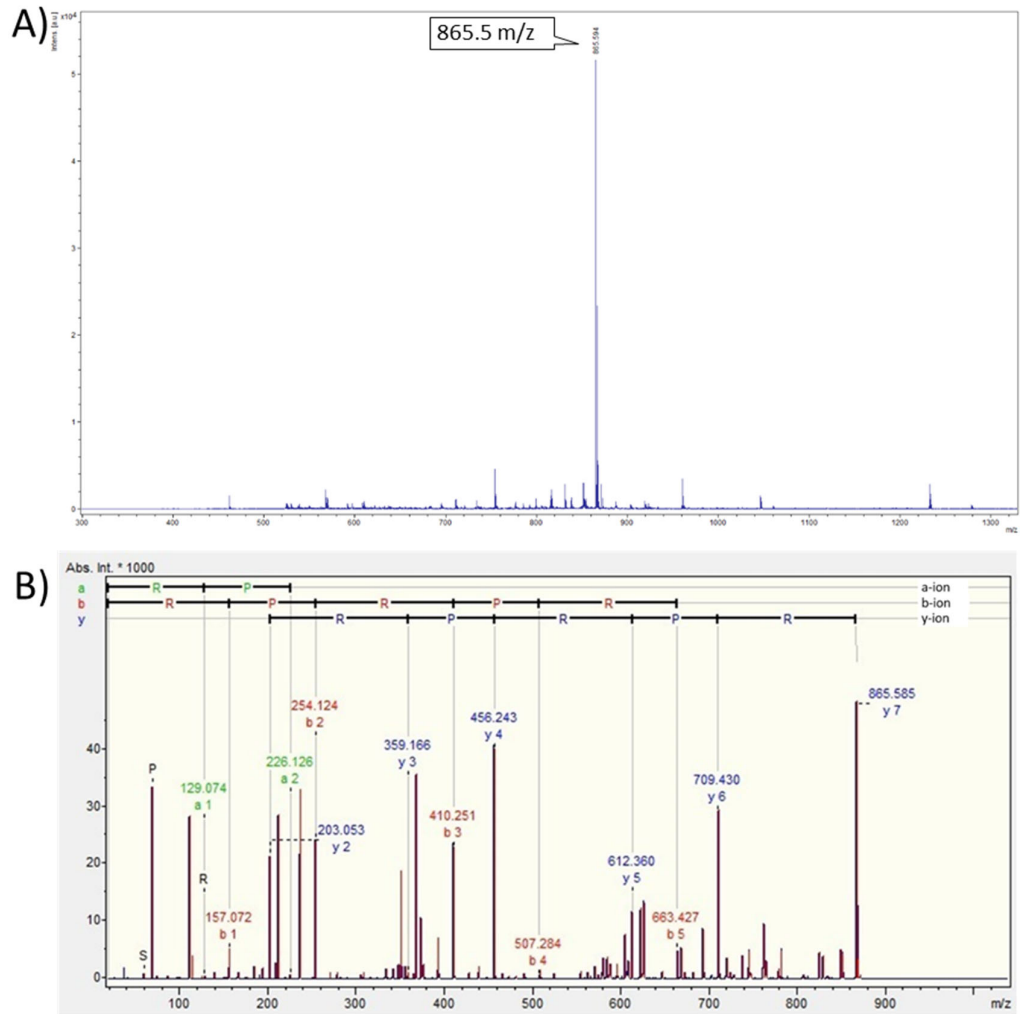


Figure S4. MS spectrum of C3-6 (A) and MS/MS identification of a peak of m/z 865.548 (B).

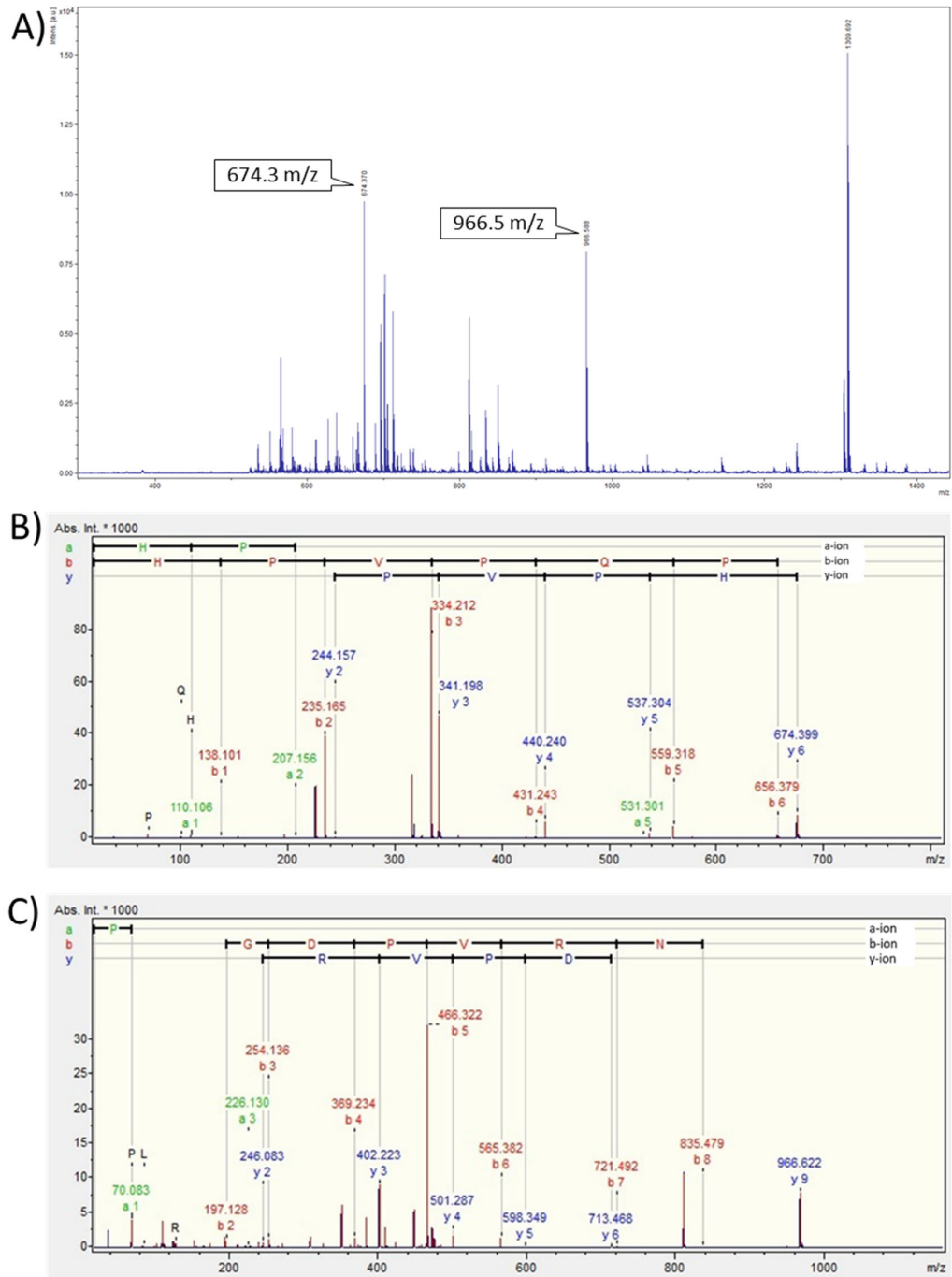


Figure S5. MS spectrum of C3-8 (A) and MS/MS identification of two peaks of m/z 674.370 (B) and 966.588 (C).

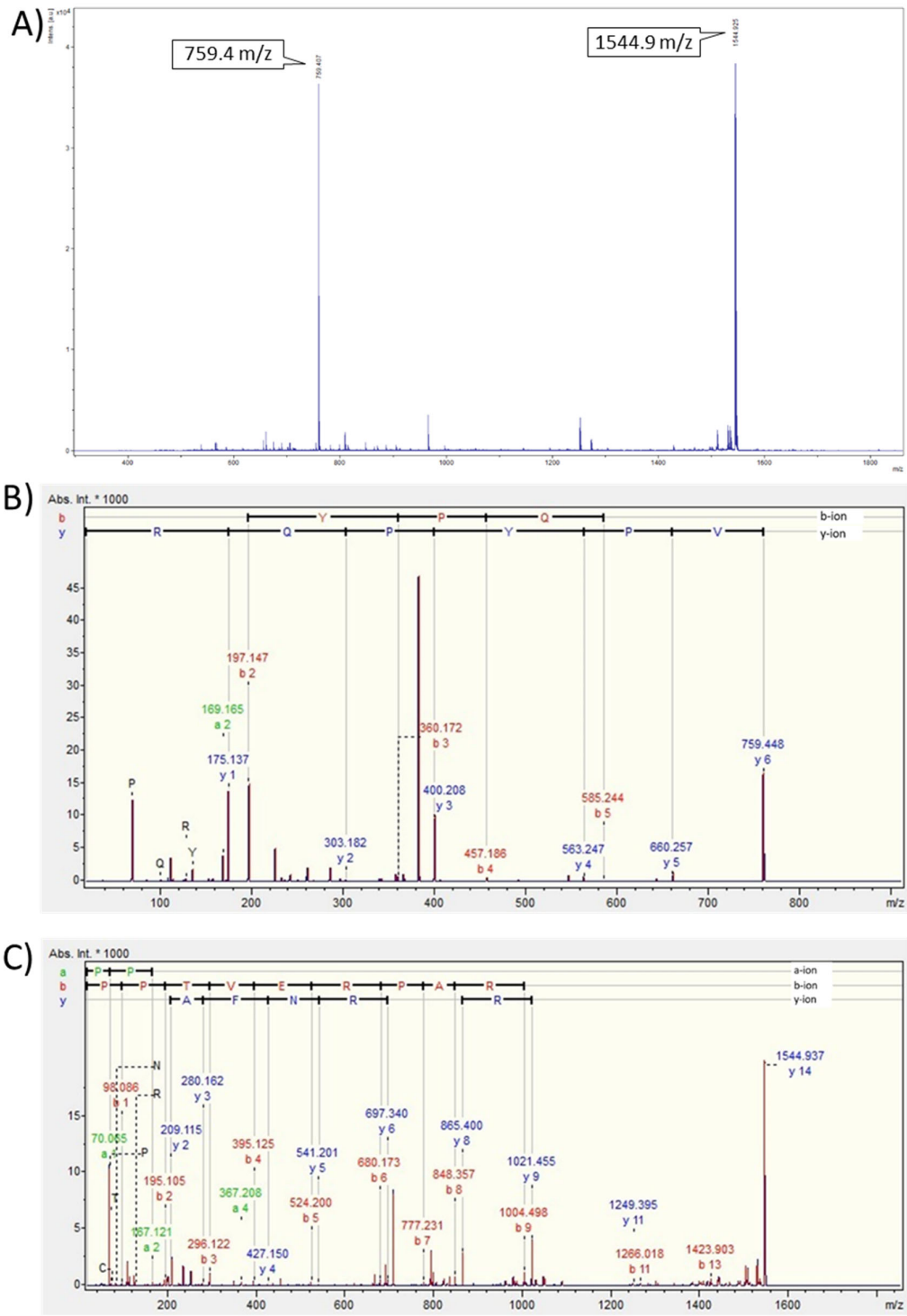


Figure S6. MS spectrum of C3-9 (A) and MS/MS identification of two peaks of m/z 759.415 (B) and 1544.925 (C).

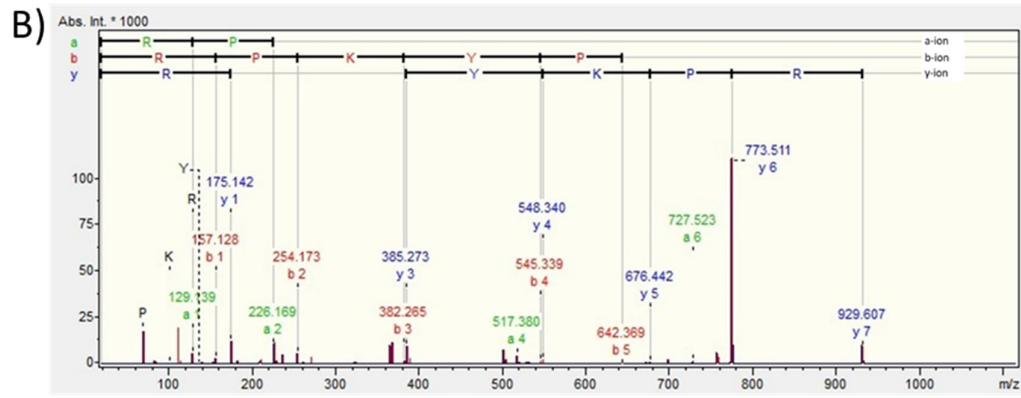
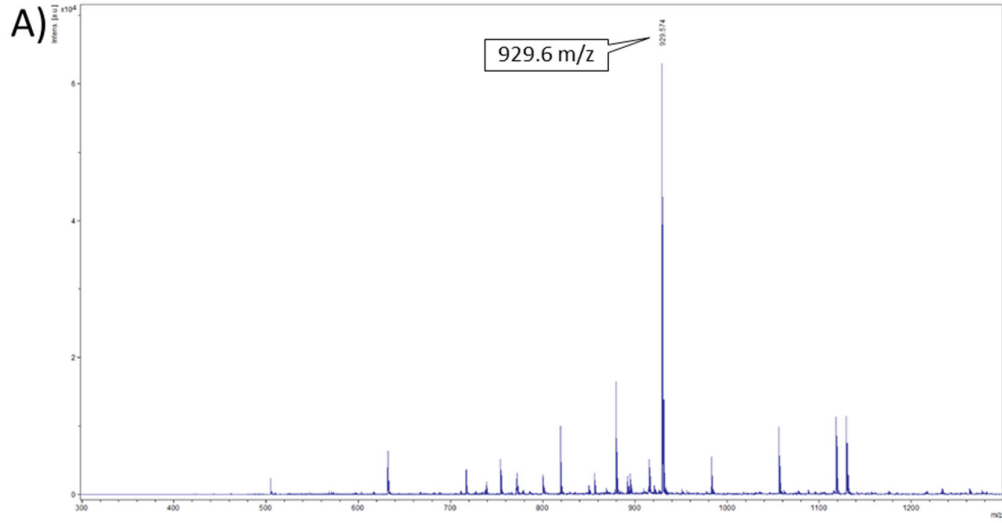


Figure S7. MS spectrum of C3-10 (A) and MS/MS identification of a peak of m/z 929.574 (B).

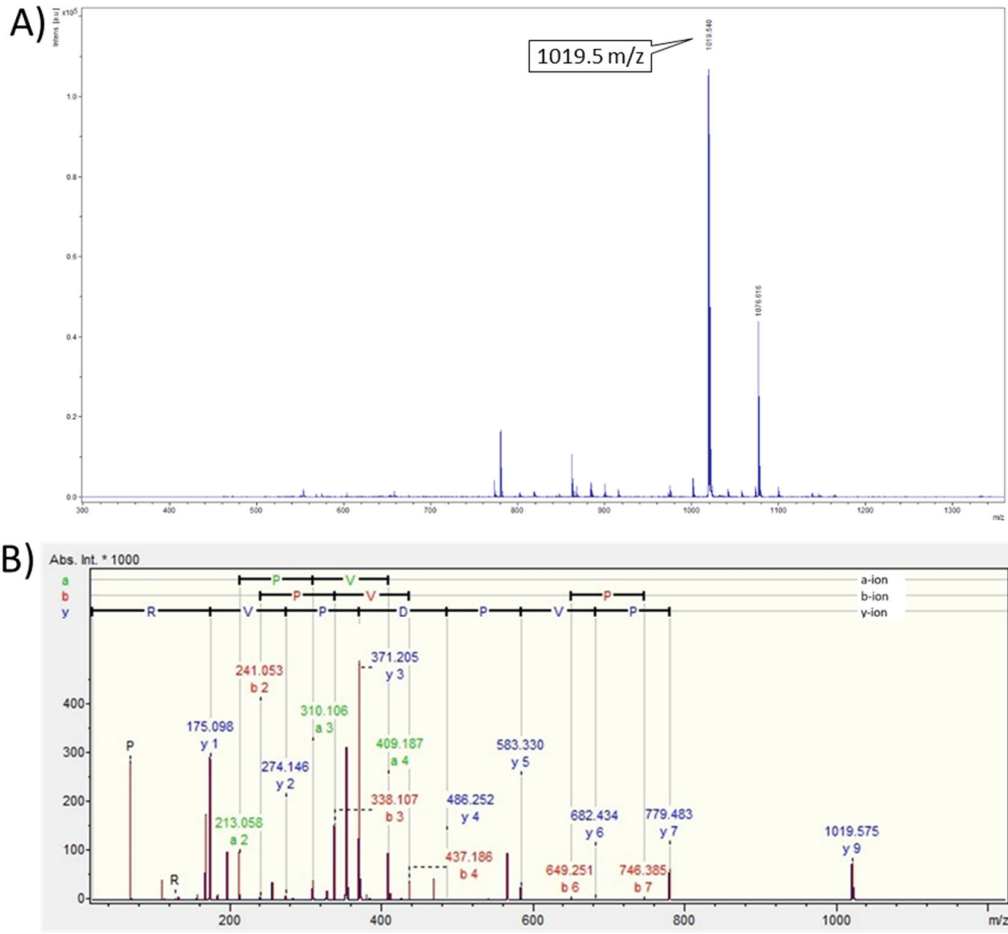


Figure S8. MS spectrum of C3-11 (**A**) and MS/MS identification of a peak of m/z 1019.540 (**B**).

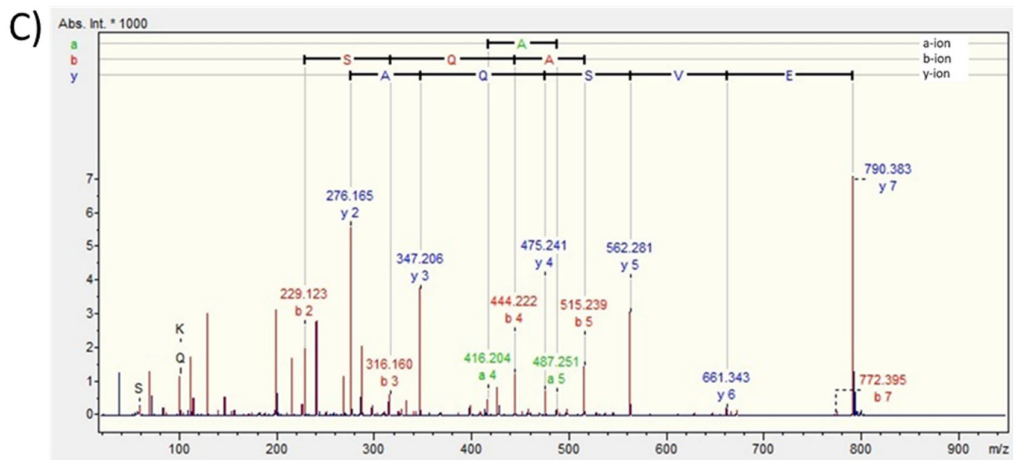
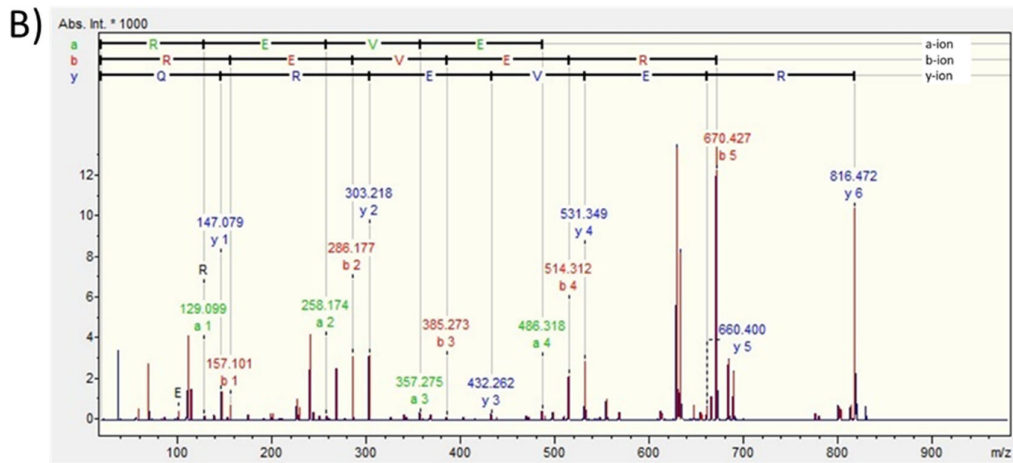
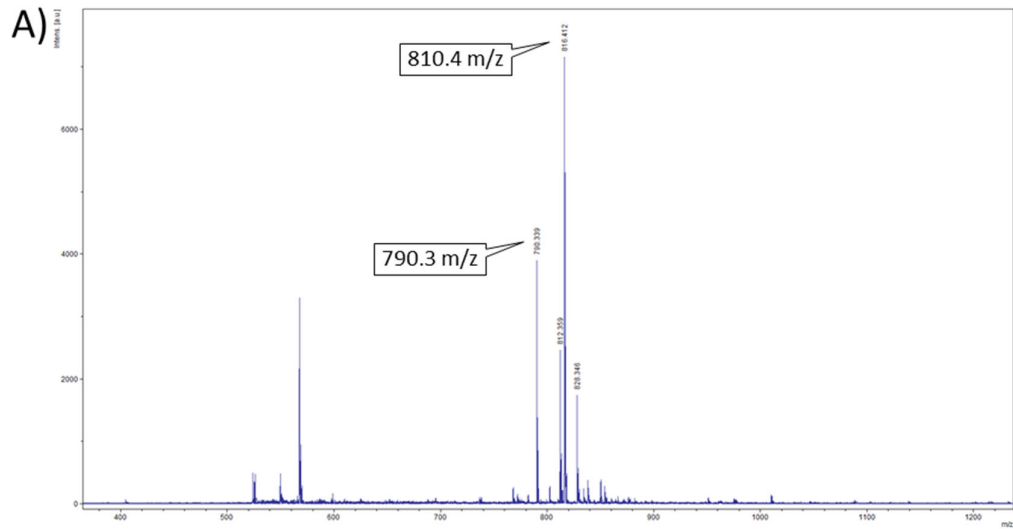


Figure S9. MS spectrum of H1-1 (A) and MS/MS identification of two peaks of m/z 816.432 (B) and 790.394 (C).

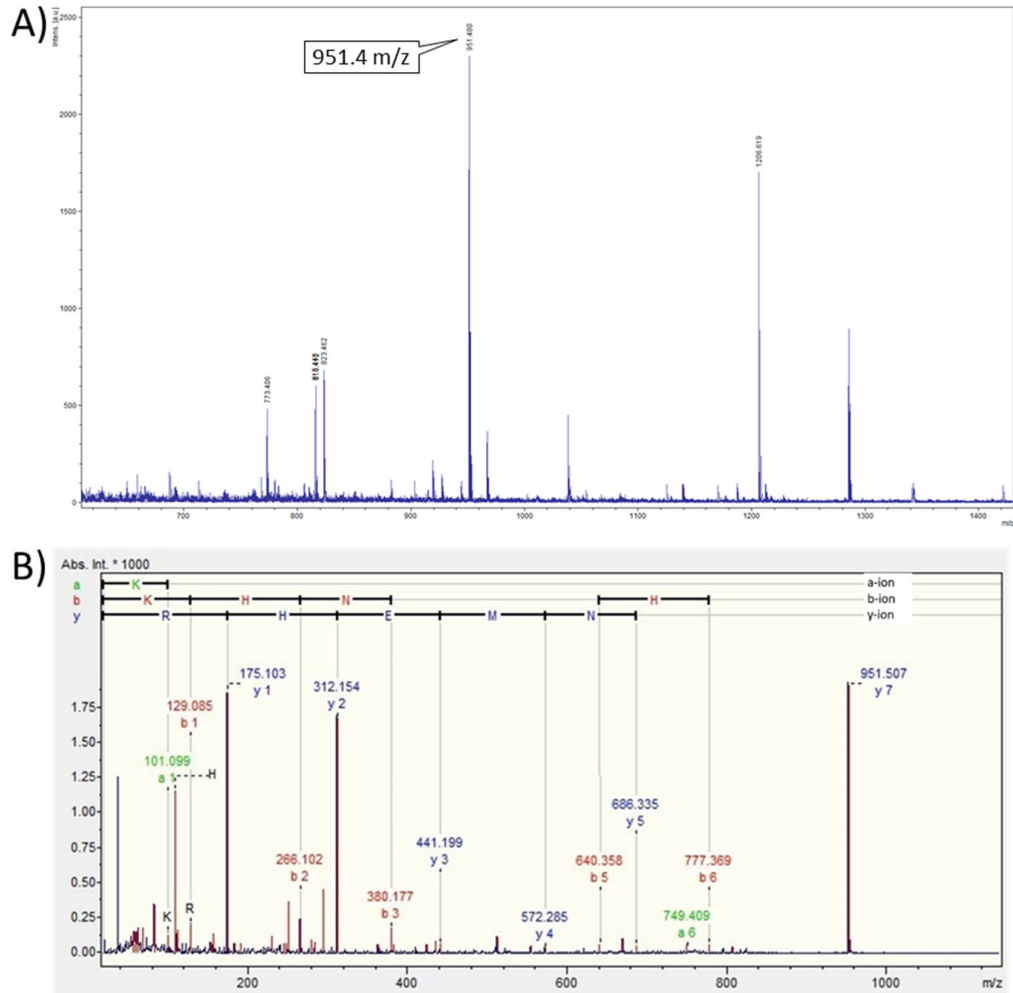


Figure S10. MS spectrum of H1-2 (A) and MS/MS identification of a peak of m/z 951.458 (B).

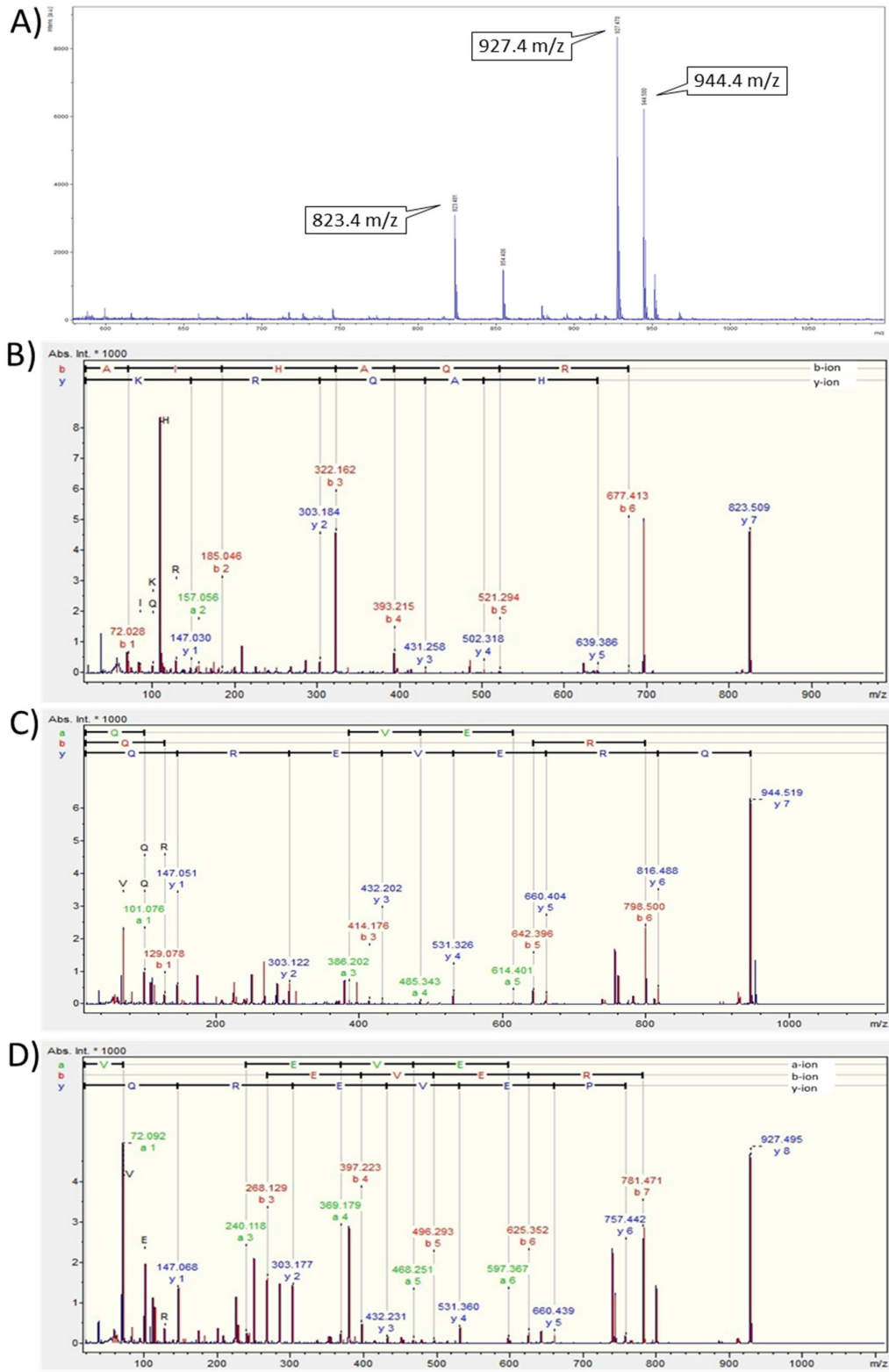


Figure S11. MS spectrum of H1-3 (A) and MS/MS identification of three peaks of m/z 823.490 (B), 944.491 (C), and 927.470 (D).

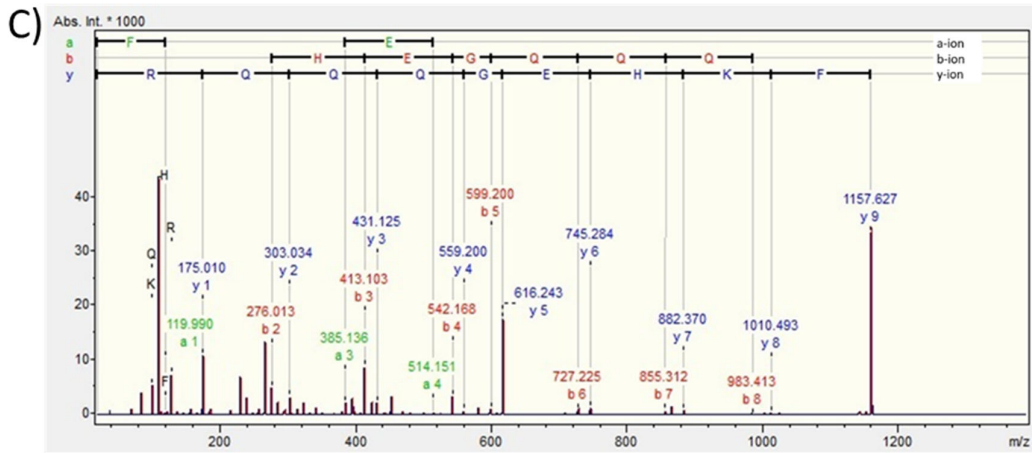
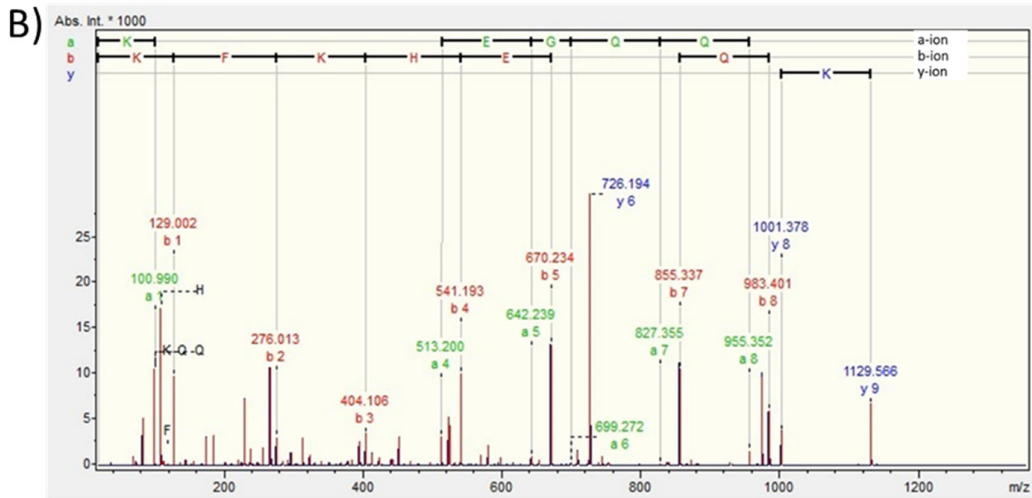
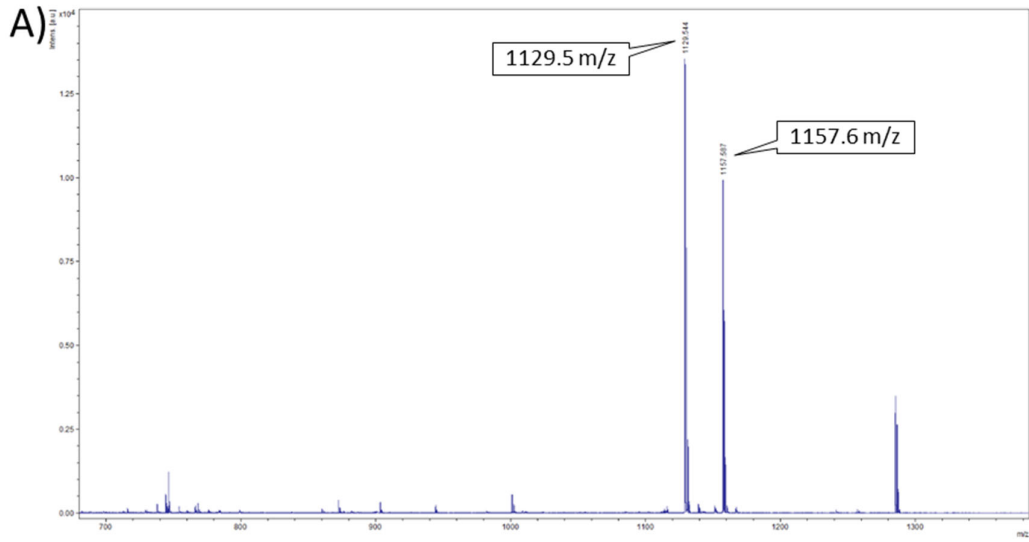


Figure S12. MS spectrum of H1-4 (A) and MS/MS identification of two peaks of m/z 1129.575 (B) and 1157.581 (C).

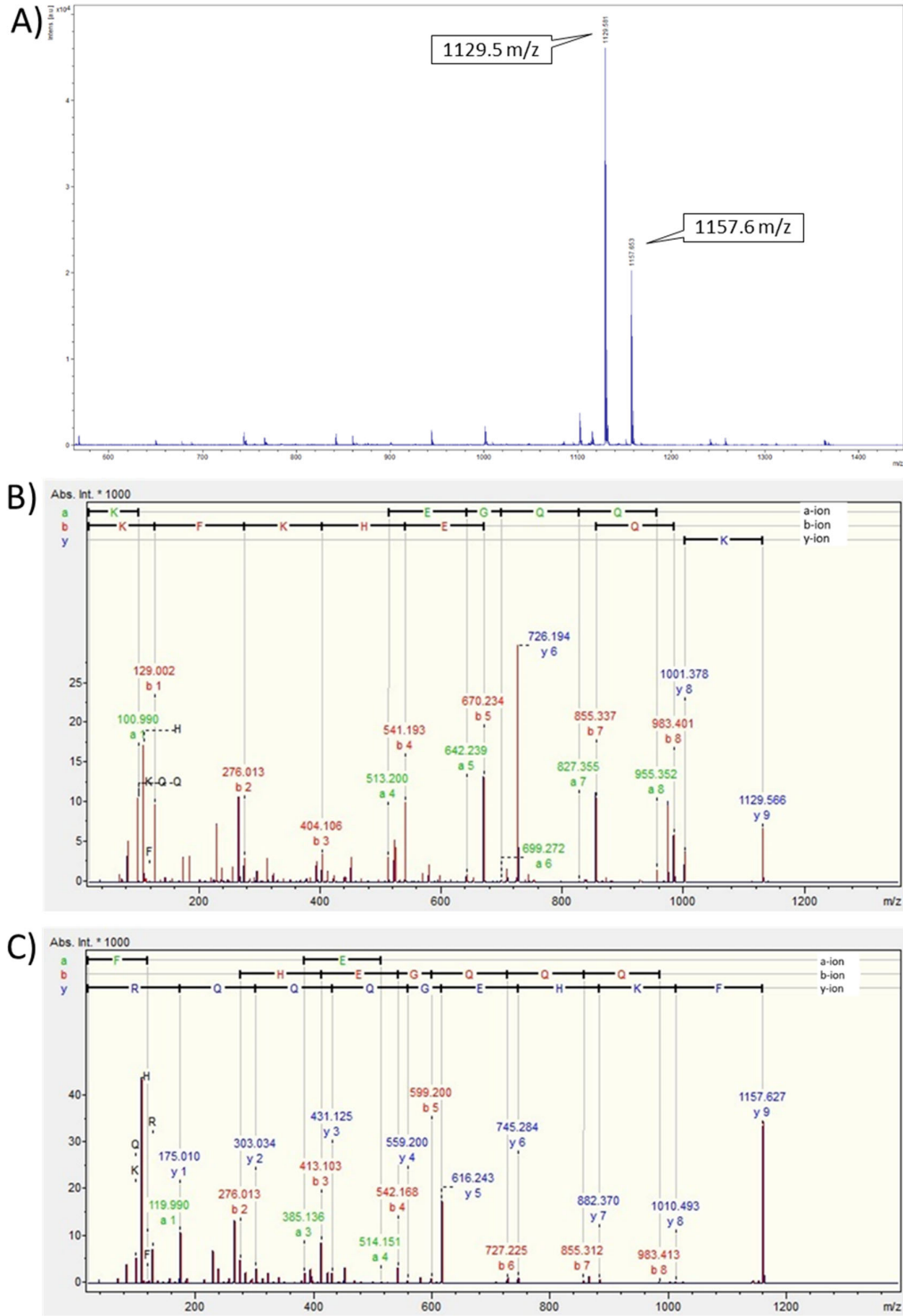


Figure S13. MS spectrum of H1-6 (A) and MS/MS identification of two peaks of m/z 1129.575 (B) and 1157.581 (C).

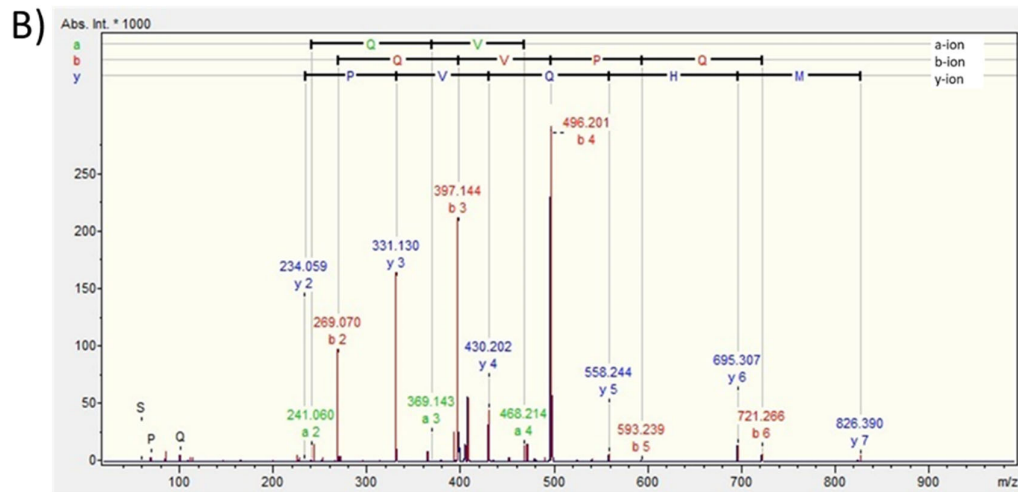
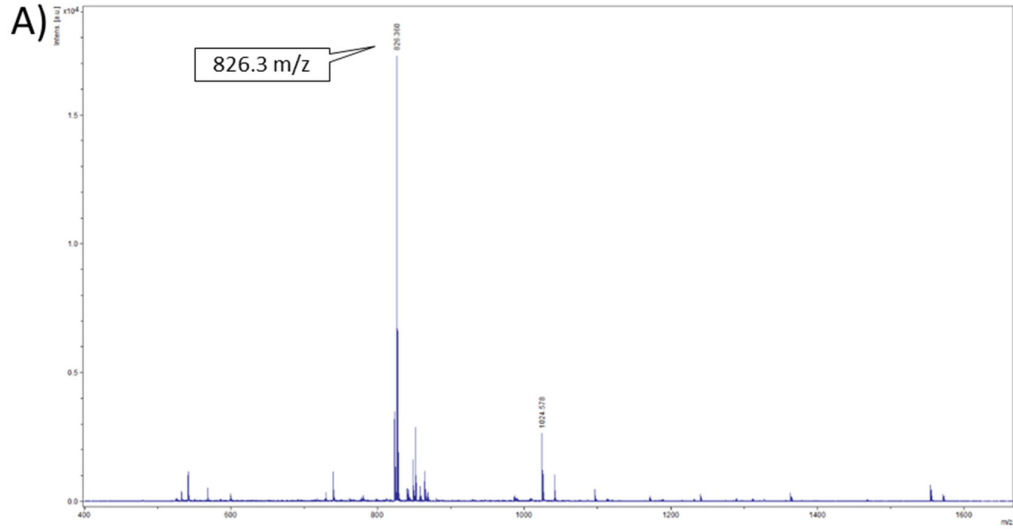


Figure S14. MS spectrum of H1-7 (A) and MS/MS identification of a peak of m/z 826.388 (B).

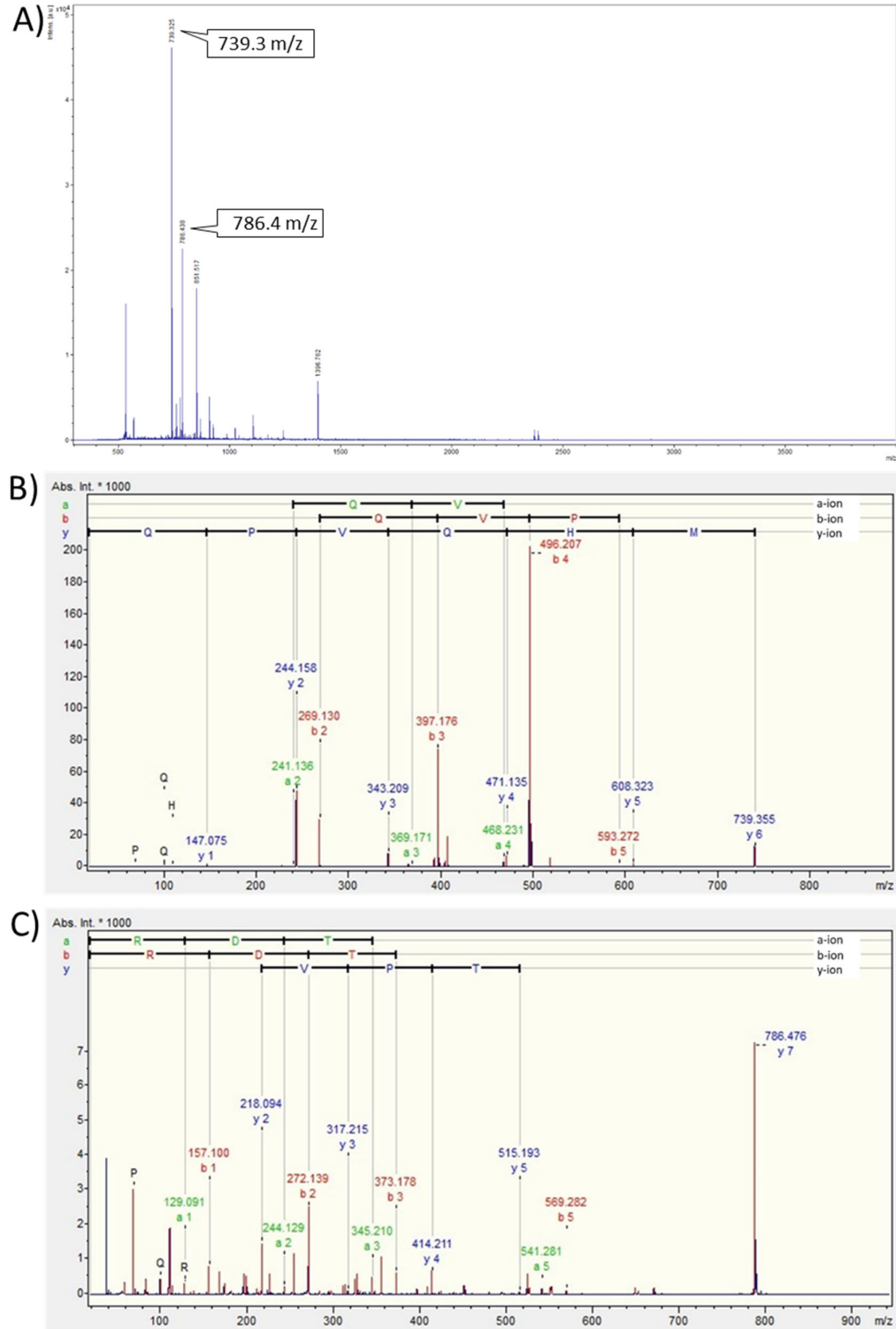


Figure S15. MS spectrum of H1-8 (A) and MS/MS identification of two peaks of m/z 739.356 (B) and 786.410 (C).

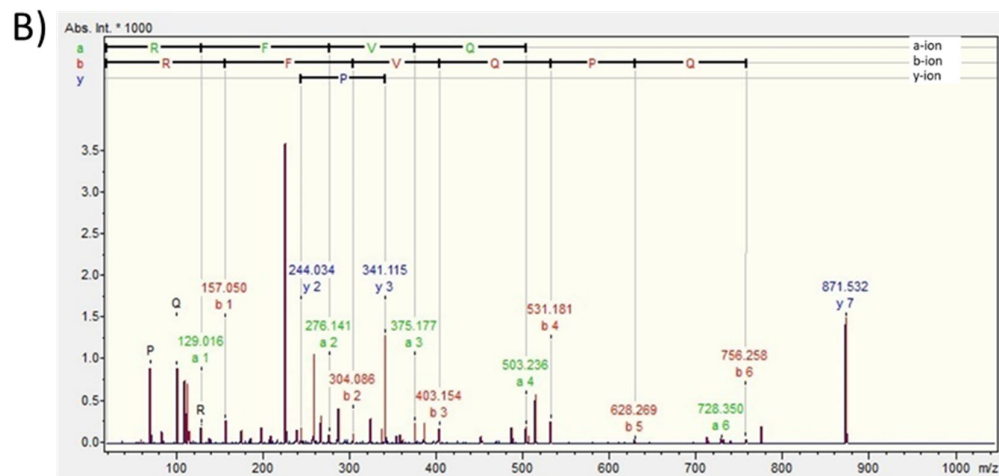
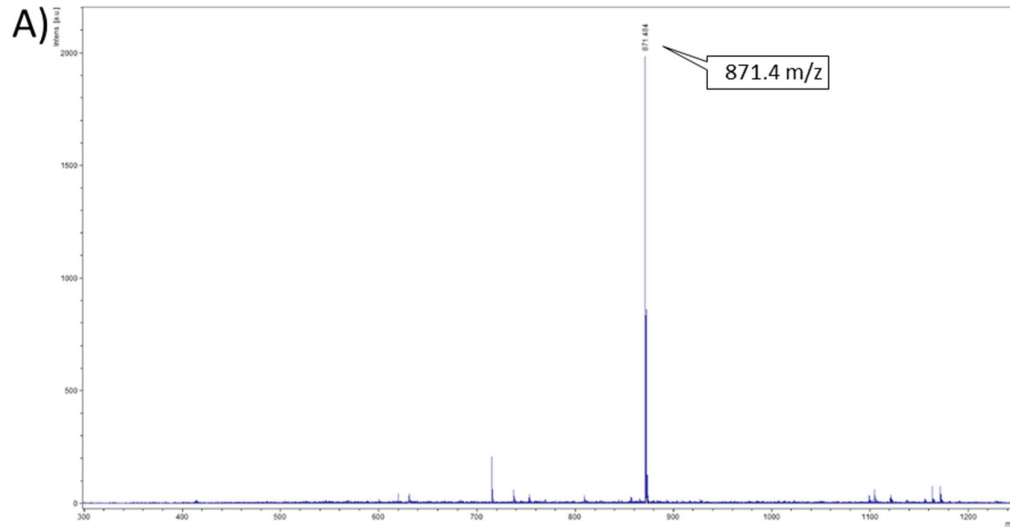


Figure S16. MS spectrum of H1-10 (A) and MS/MS identification of a peak of m/z 871.484 (B).

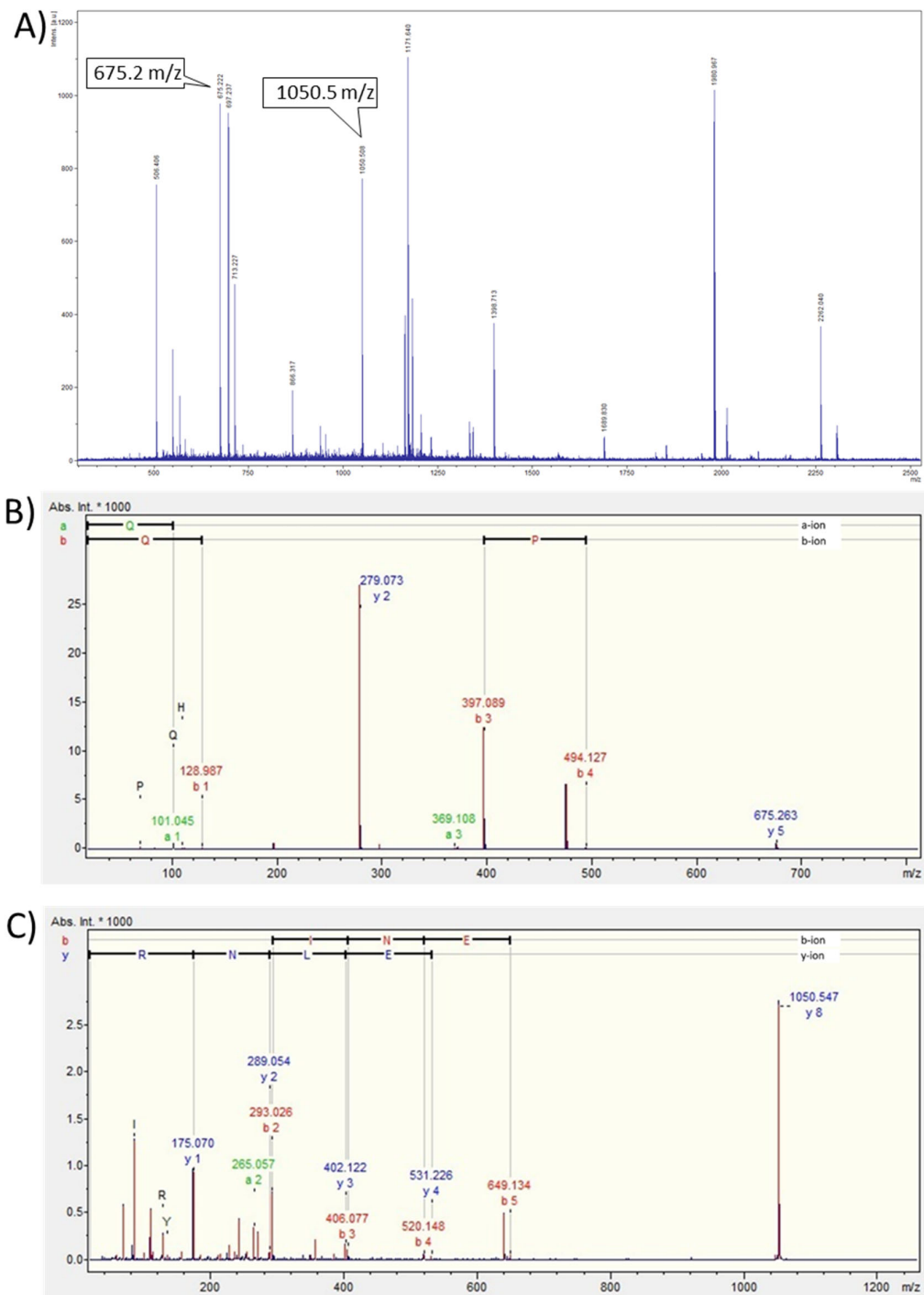


Figure S17. MS spectrum of H1-13 (A) and MS/MS identification of two peaks of m/z 675.222 (B) and 1050.508 (C).

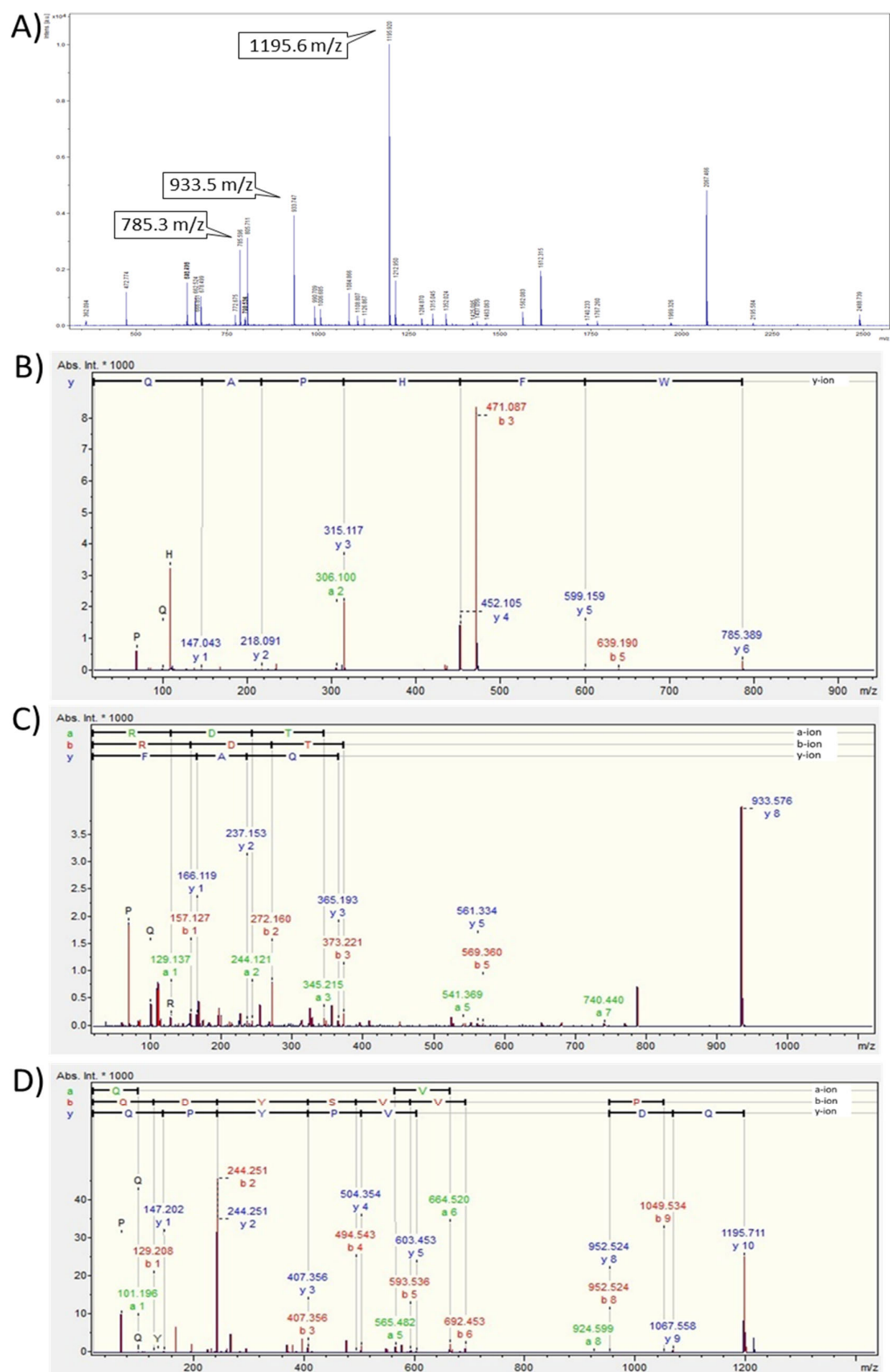


Figure S18. MS spectrum of H1-14 (A) and MS/MS identification of three peaks of m/z 785.358 (B), 933.512 (C), and 1195.652 (D).

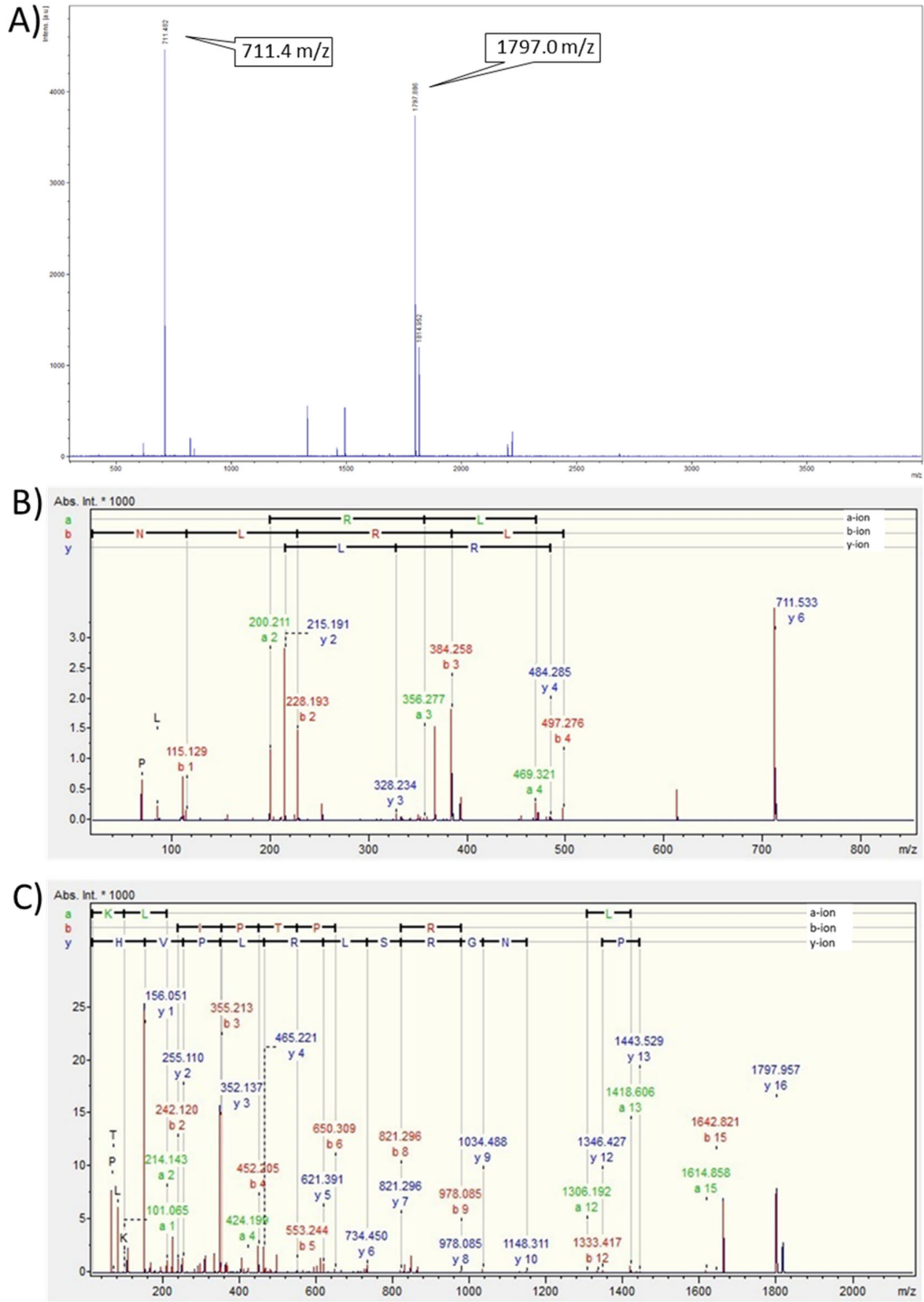


Figure S19. MS spectrum of H1-19 (A) and MS/MS identification of two peaks of m/z 711.451 (B) and 1797.000 (C).

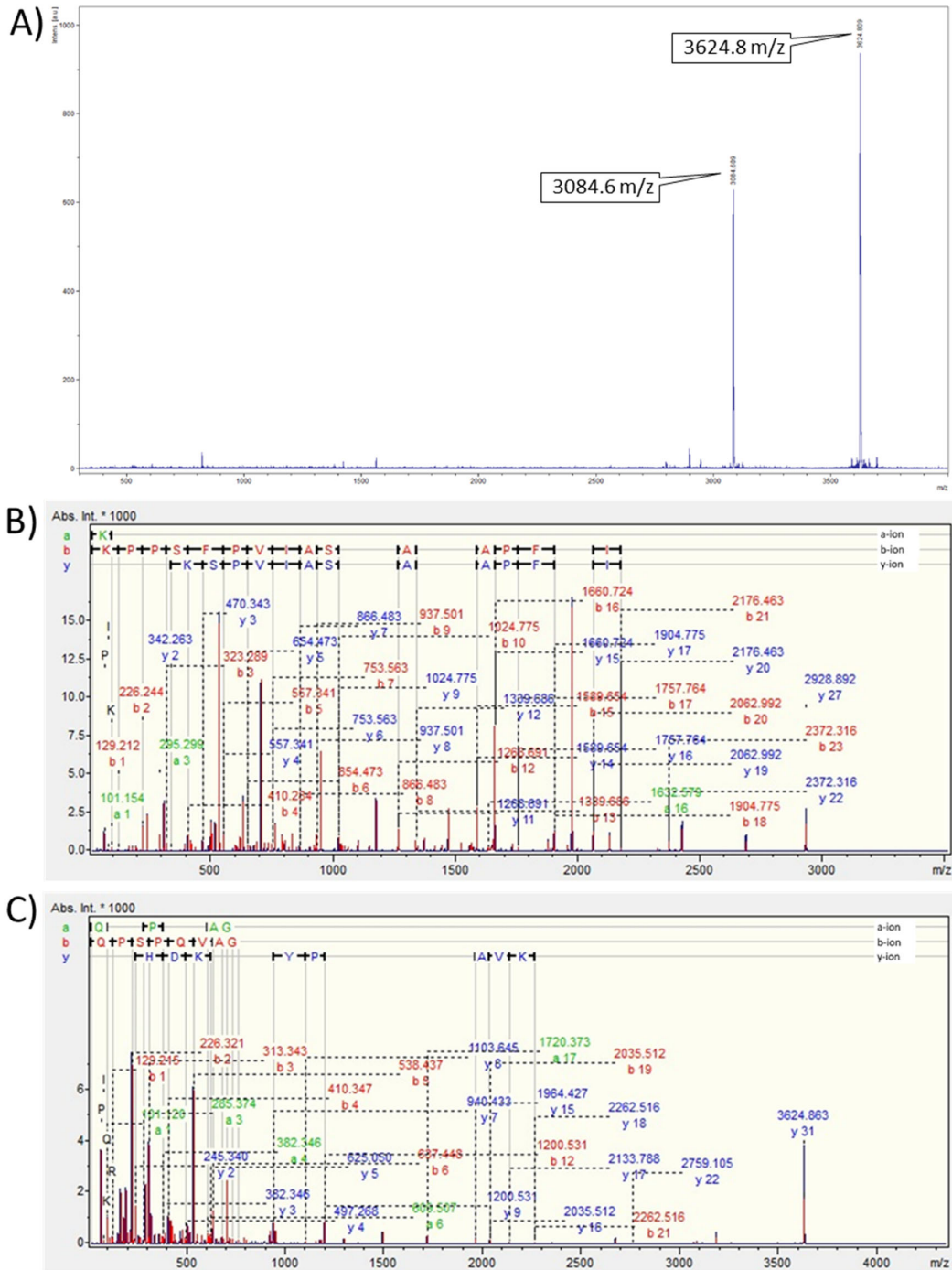


Figure S20. MS spectrum of H1-20 (A) and MS/MS identification of two peaks of m/z 3084.609 (B) and 3624.809 (C).

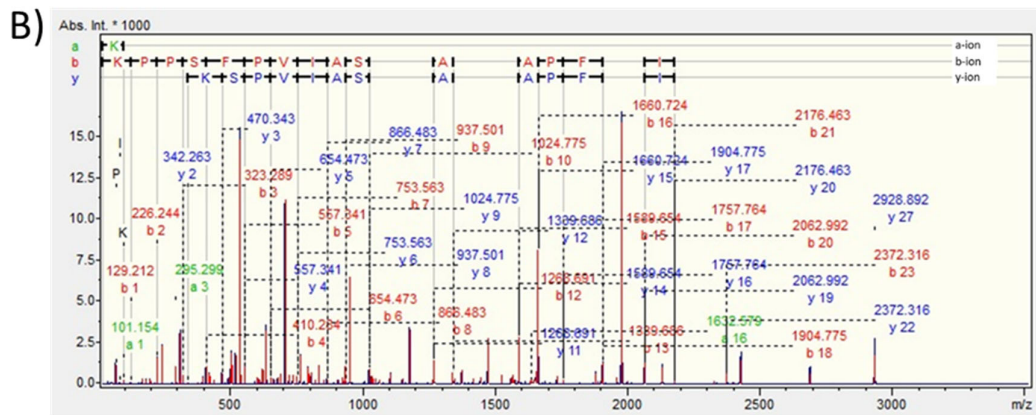
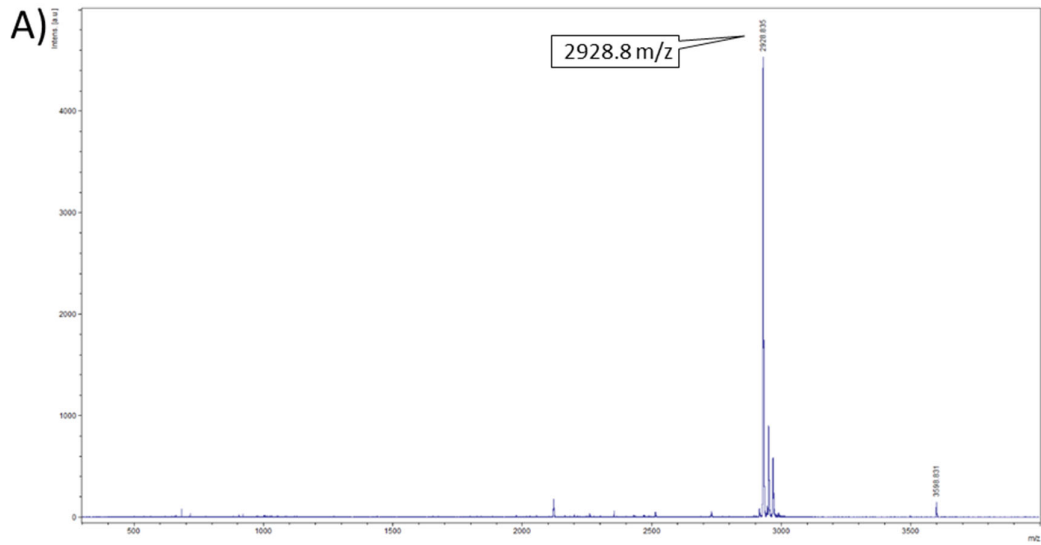


Figure S21. MS spectrum of H1-21 (A) and MS/MS identification of a peak of m/z 2928.835 (B).

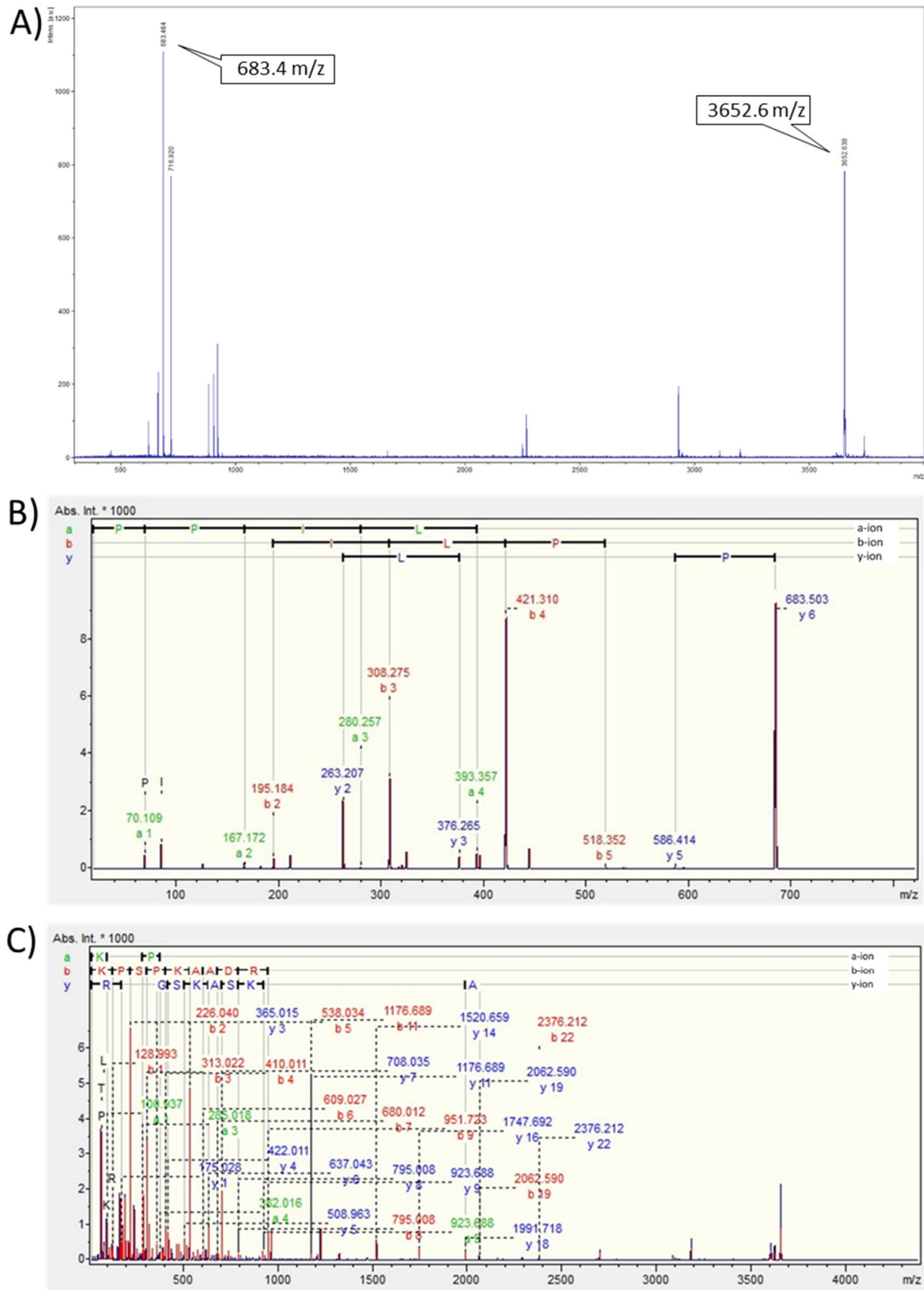


Figure S22. MS spectrum of H1-22 (A) and MS/MS identification of two peaks of m/z 683.468 (B) and 3652.638 (C).